Decorating Mesoporous Silicon with Amorphous Metal-Phosphorous-derived Nanocatalysts towards Enchanced Photoelectrochemical Water Reduction

Hefeng Zhang[a,b], Ailong Li[a,b], Zhiliang Wang[a,b], Weiguang Ma[a], Deng Li[a,b], Xu Zong[a]* and Can Li[a]*

[a]State Key Laboratory of Catalysis, Dalian Institute of Chemical Physics, Chinese Academy of Sciences, Dalian National Laboratory for Clean Energy, The Collaborative Innovation Center of Chemistry for Energy Materials (iChEM), Zhongshan Road 457, Dalian, 116023, China

[b]University of Chinese Academy of Sciences, Beijing, 100049, China

*Correspondence and requests for materials should be addressed to C. L. and X. Z.

Email: canli@dicp.ac.cn; xzong@dicp.ac.cn

Phone: (86)-411-84379070; (86)-411-84379698

Address: State Key Laboratory of Catalysis, Dalian Institute of Chemical Physics, Chinese Academy of Science, Dalian, Liaoning Province 116023, China

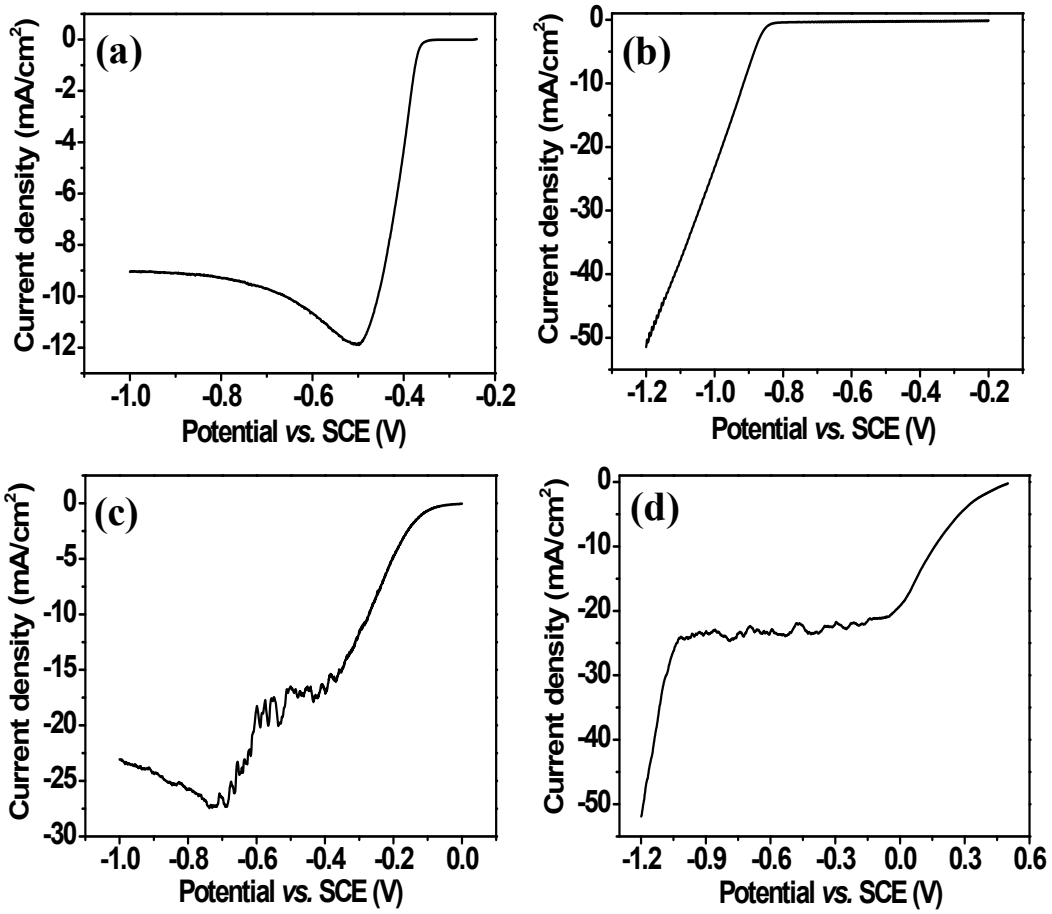

Fig. S1 Current-potential curves for the photo-assisted electrodeposition of (a) Ni-P, (c) Fe-P on Bp-Si photocathodes under simulated AM 1.5 solar irradiation (100 mW cm^{-2}). Current-potential curves for the electrodeposition of (b) Ni-P, (d) Fe-P on graphite electrode.

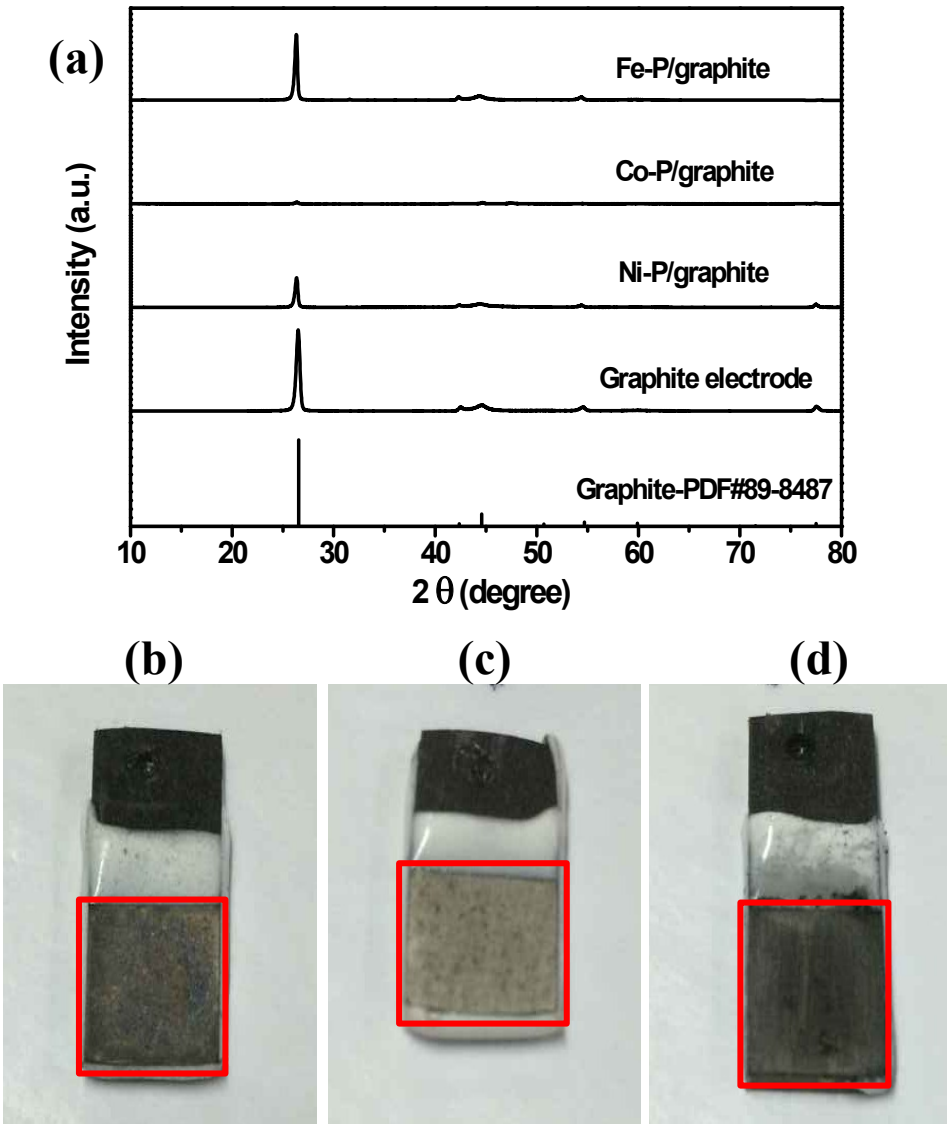
(a)
Fe-P/graphite
Co-P/graphite
Ni-P/graphite
Graphite electrode
Graphite-PDF#89-8487
Intensity (a.u.)
10
20
30
40
50
60
70
80
2 θ (degree)
(b)
(c)
(d)

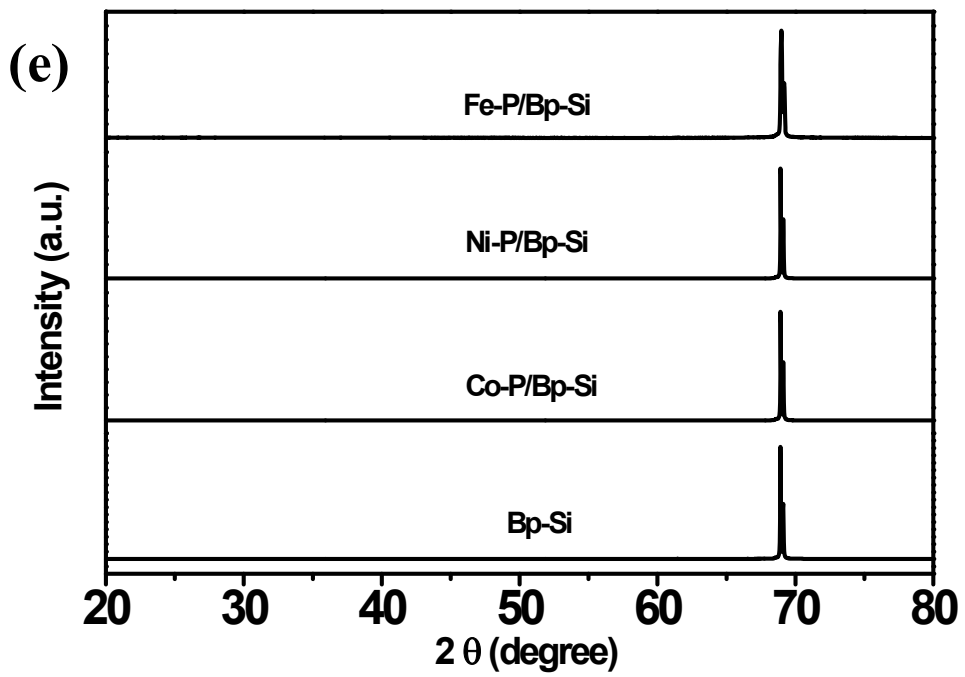

Fig. S2 (a) XRD patterns of graphite, Fe-P/graphite, Co-P/graphite, and Ni-P/graphite electrodes. The standard XRD pattern of graphite is also shown as a reference. The M-Ps/graphite electrodes were prepared by electrodeposition method. Photographs of (b) Co-P/graphite, (c) Ni-P/graphite, and (d) Fe-P/graphite electrodes, respectively. The area for the deposition of M-Ps is referred by the red frame. The photographs showed that the Co-P and Ni-P films were thick, while the Fe-P film was thin, which can explain the varied intensity of the XRD peaks of graphite for M-Ps/graphite electrodes. (e) XRD patterns of Bp-Si, Co-P/Bp-Si, Ni-P/Bp-Si and Fe-P/Bp-Si. Bp-Si exhibited one dominated peak indexed to (400) crystal facet due to [100] crystal orientation of the used Si wafer.

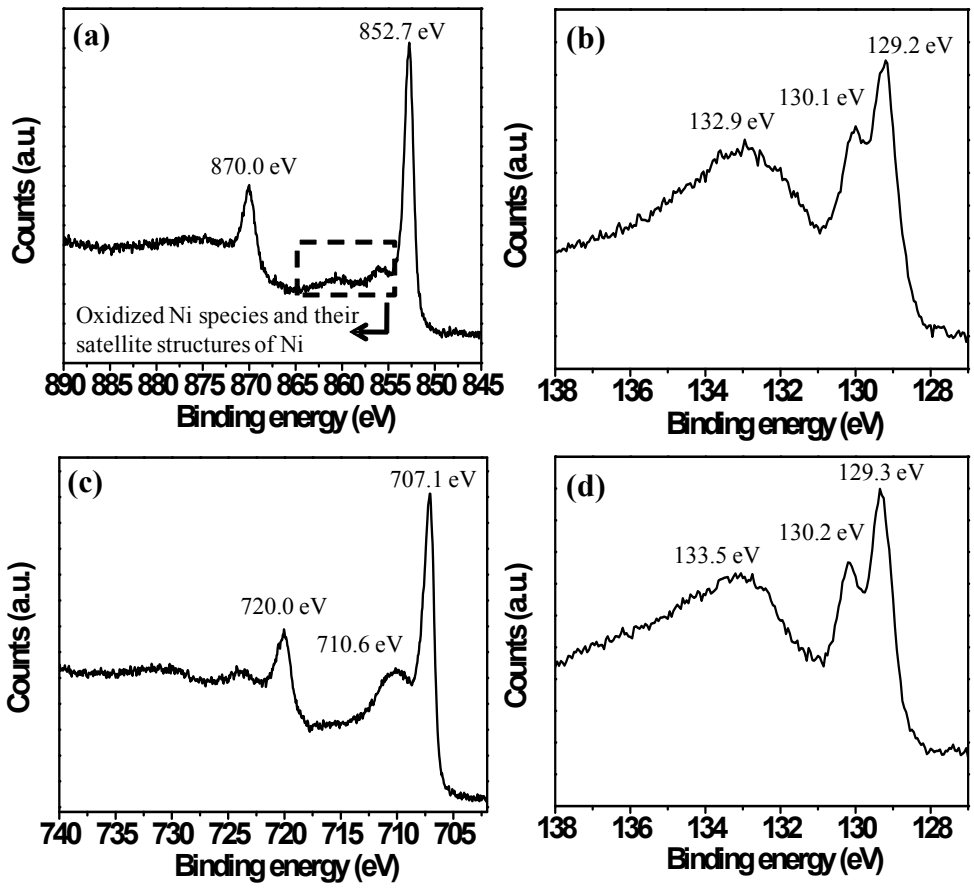

Fig. S3 XPS spectra of the M-Ps/Bp-Si after LSV test. (a) Ni 2p region of Ni-P, (b) P 2p region of Ni-P, (c) Fe 2p region of Fe-P, (d) P 2p region of Fe-P. The peaks in Fig. S3a for the BE of Ni $2p_{3/2}$ and $2p_{1/2}$ appear at 852.7 and 870.0 eV, respectively. All of the other peaks are assigned to oxidized Ni species and their satellite structures.[1] The high-resolution P 2p region (Fig. S3b) shows two peaks at 130.1 and 129.2 eV, assigned to the BE of P $2p_{1/2}$ and $2p_{3/2}$, respectively, along with one peak at 132.9 eV corresponding to oxidized P species.[1] In addition, Fig. S3c shows two peaks at 707.1 and 720.0 eV associated with Fe $2p_{3/2}$ and $2p_{1/2}$, respectively, whereas the peak at 710.6 eV reflects the BE of oxidized Fe species.[2, 3] For the high-resolution P 2p region (Fig. S3d), peaks at 129.3, 130.2 and 133.5 eV can be assigned to P $2p_{3/2}$, P $2p_{1/2}$ and oxidized P species, respectively.[2, 3]

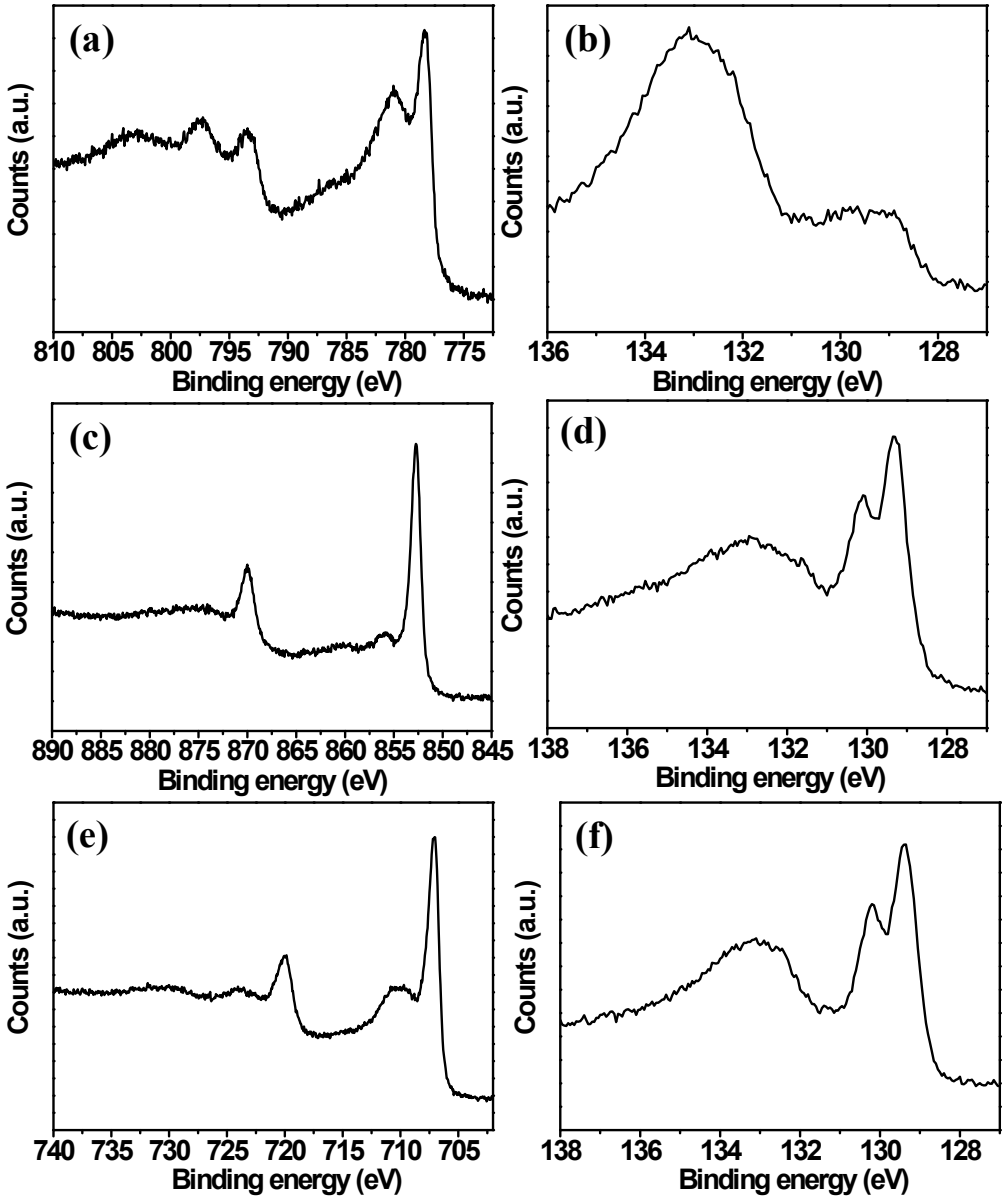

Fig. S4 XPS spectra of the M-Ps/Bp-Si before LSV test. (a) Co 2p region of Co-P, (b) P 2p region of Co-P, (c) Ni 2p region of Ni-P, (d) P 2p region of Ni-P, (e) Fe 2p region of Fe-P and (f) P 2p region of Fe-P.

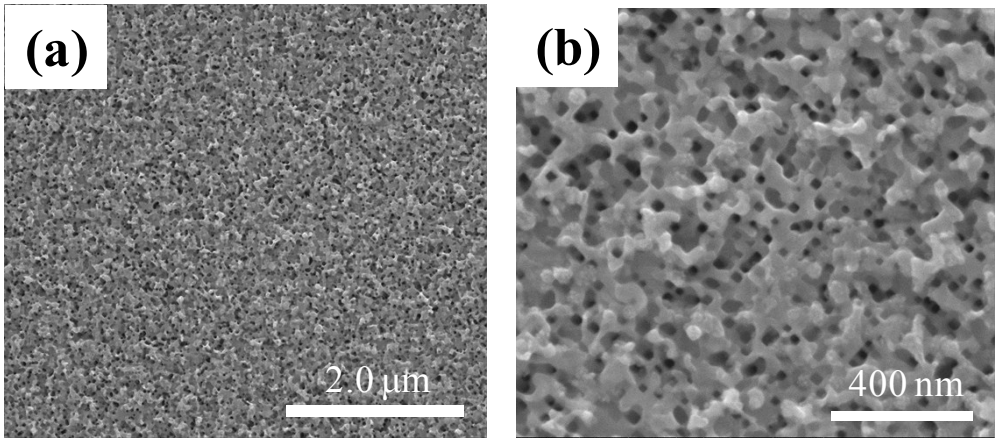

Fig. S5 Top-view SEM images of Ni-P/Bp-Si with different scale bars.

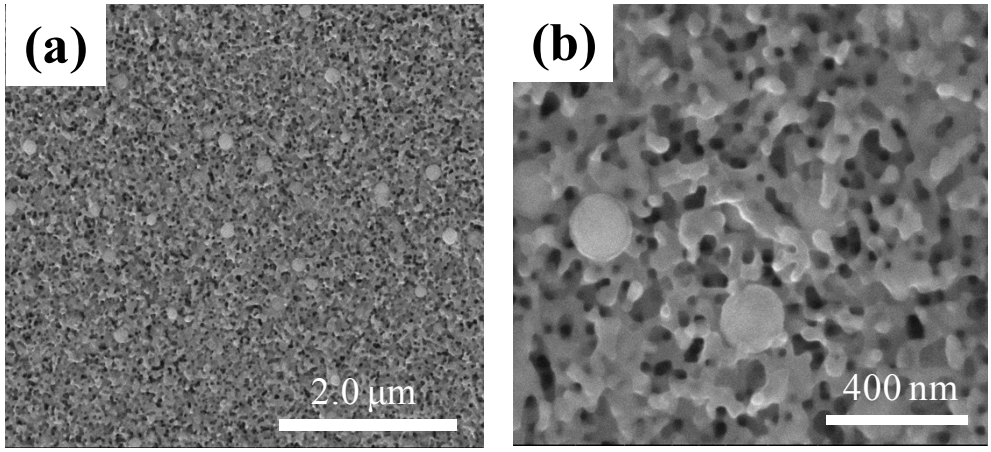

Fig. S6 Top-view SEM images of Fe-P/Bp-Si with different scale bars.

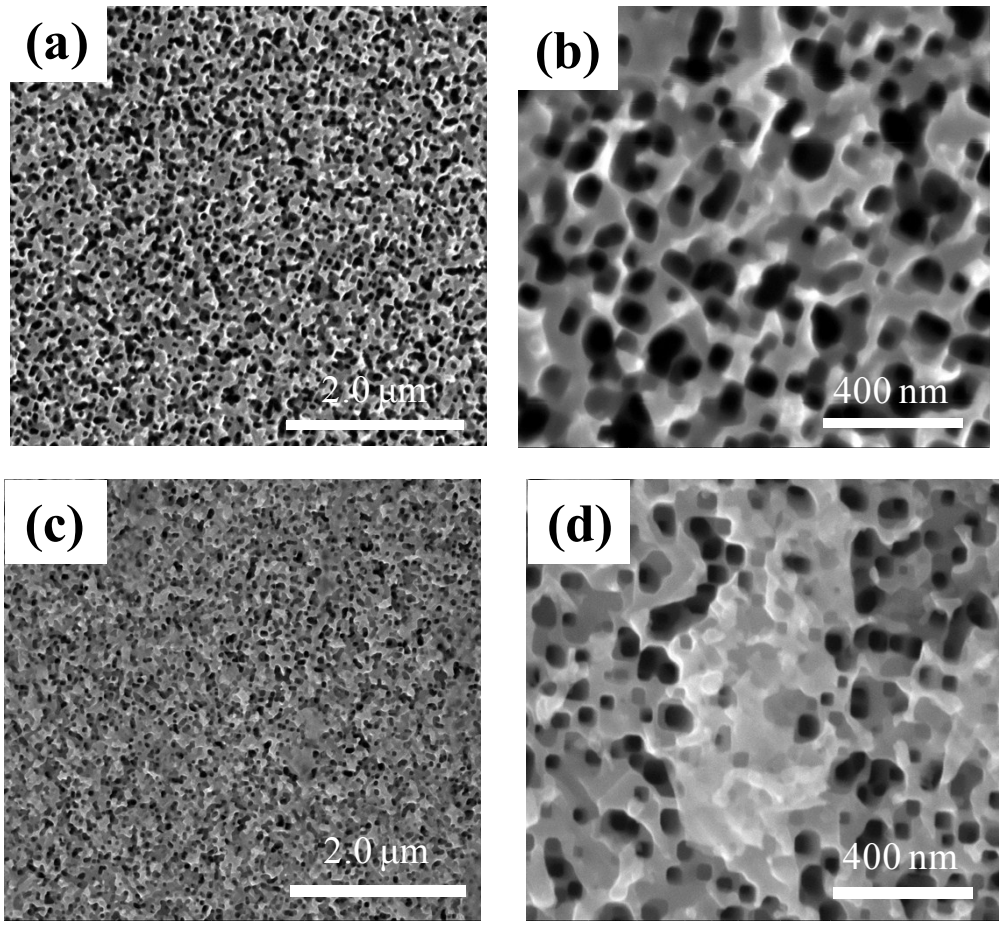

Fig. S7 Top-view SEM images of (a) and (b) Bp-Si; (c) and (d) Co-P/Bp-Si with different scale bars.

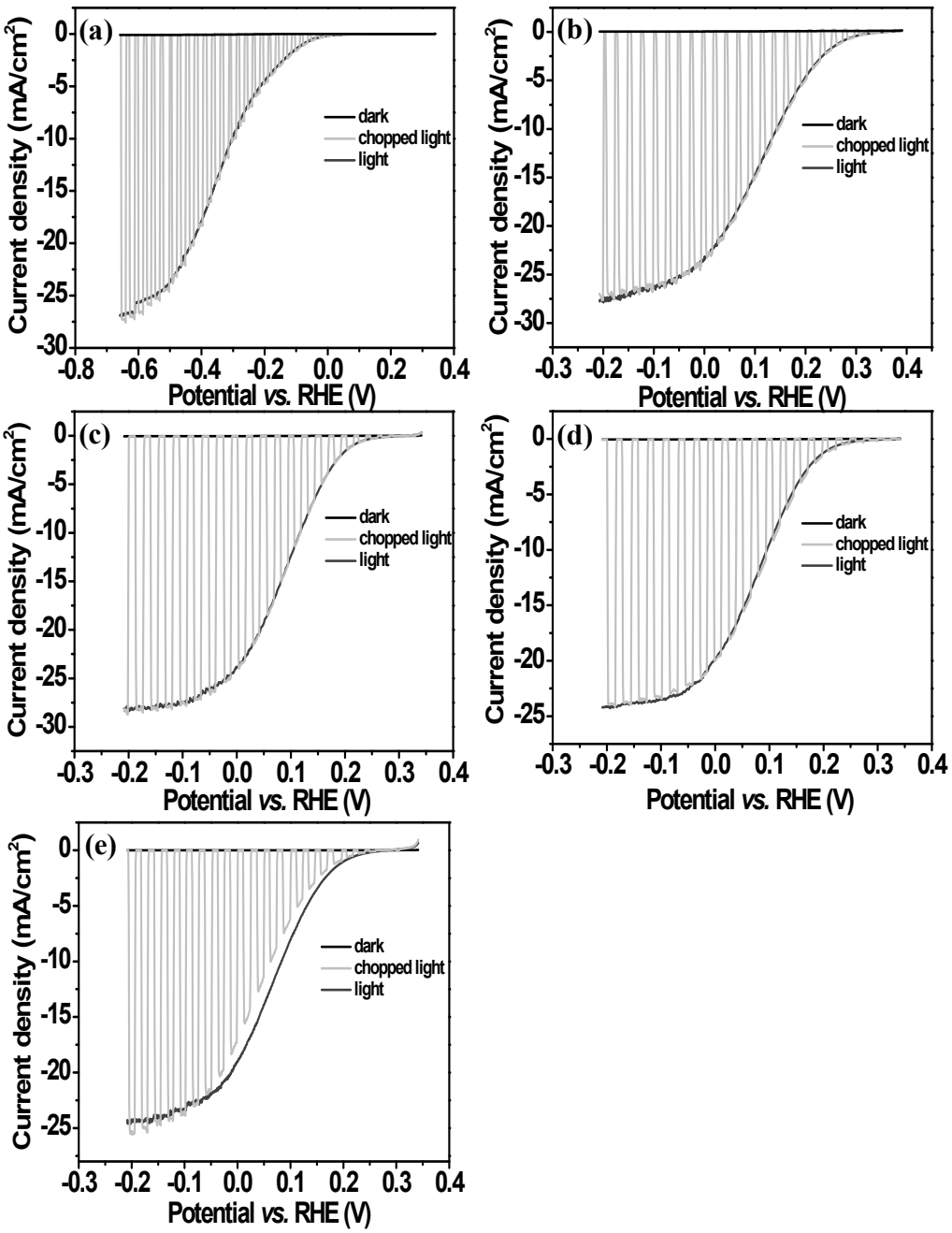

Fig. S8 Current-potential curves of (a) Bp-Si, (b) Pt/Bp-Si, (c) Co-P/Bp-Si, (d) Ni-P/Bp-Si, and (e) Fe-P/Bp-Si photoeletrodes. Conditions: AM 1.5G simulated sunlight (100 mW cm^{-2}), 0.5 M H_2SO_4 as electrolyte, Ar was used to expel air in the electrolyte.

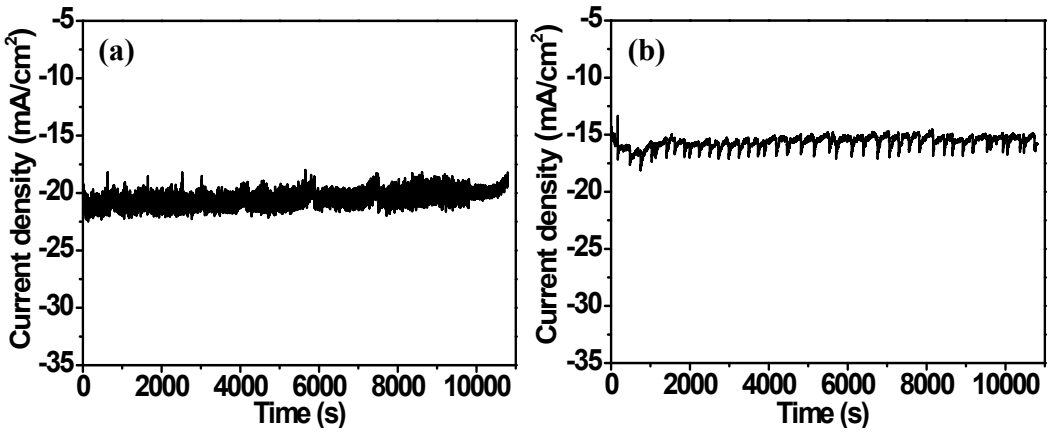

Fig. S9 Chronoamperometry measurement on (a) Ni-P/Bp-Si, and (b) Fe-P/Bp-Si photocathodes at 0 V *vs.* RHE under AM 1.5G illumination (100 mW cm^{-2}) in 0.5 M H_2SO_4 aqueous solution.

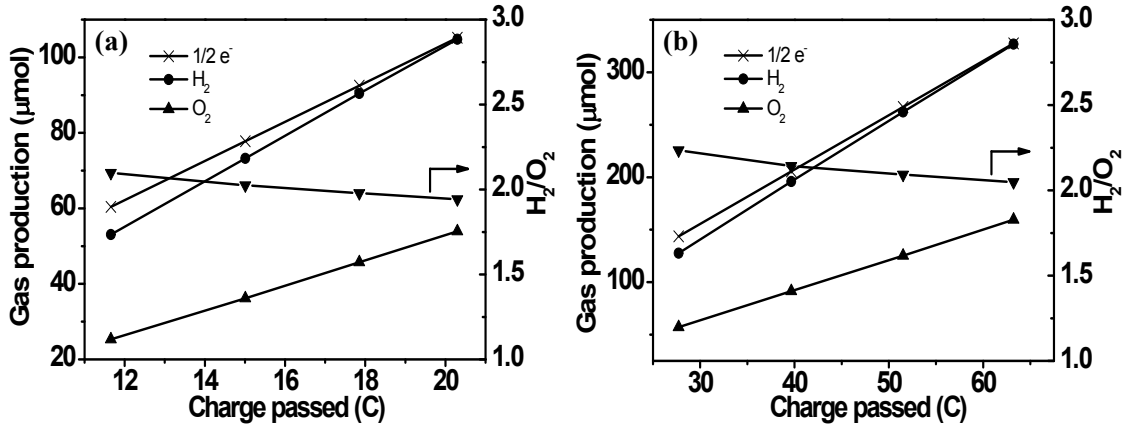

Fig. S10 Hydrogen and oxygen evolution using (a) Ni-P/Bp-Si, (b) Fe-P/Bp-Si as photocathodes, Pt as the counter electrode, and SCE as the reference electrode in 0.5 M H_2SO_4 solution at an applied bias of 0 V *vs.* RHE under 300 W Xe light irradiation.

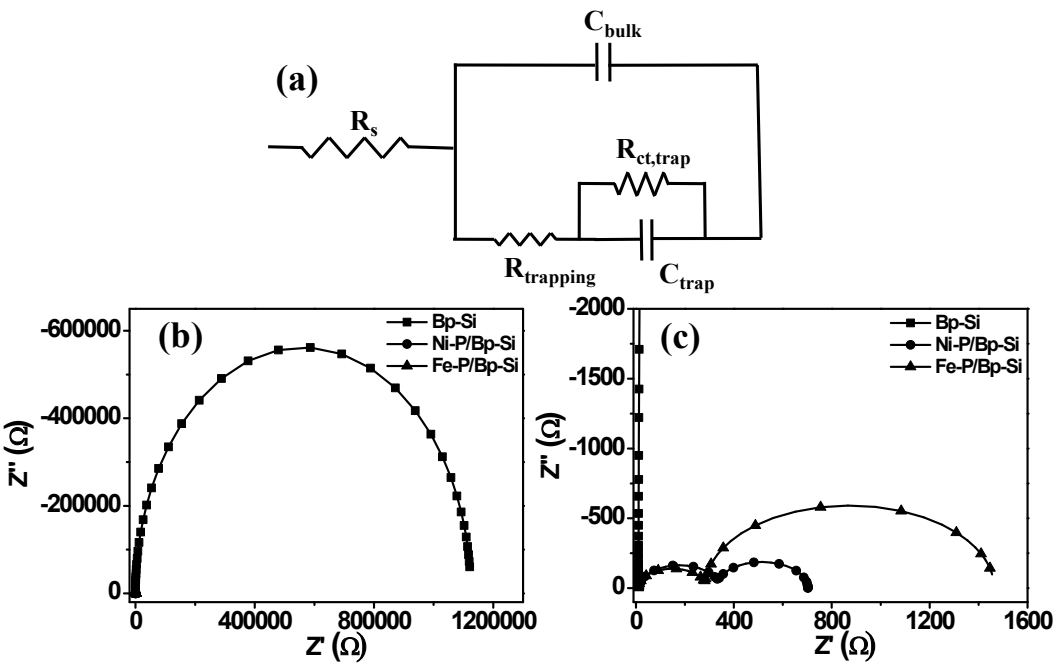

Fig. S11 (a) Equivalent circuit used to fit the impedance data consisted of a series resistance (R_s), a capacitance of Si (C_{bulk}), a capacitance of catalyst (C_{trap}), a resistance of the charge transfer from Si to catalyst ($R_{trapping}$), and a resistance of the charge transfer from catalyst to electrolyte($R_{ct,trap}$). [4] (b) Nyquist plots, and (c) magnified Nyquist plots of Bp-Si, Ni-P/Bp-Si and Fe-P/Bp-Si recorded at +0.28 V *vs.* RHE in 0.5 M H_2SO_4 aqueous solution under AM 1.5G illumination (100 mW cm^{-2}).

Table S1 Fitting parameters obtained by fitting the Nyquist plots using the equivalent circuit in Fig. S11a.

Samples	R_s (Ω)	C_{bulk} (F)	$R_{trapping}$ (Ω)	C_{trap} (F)	$R_{ct,trap}$ (Ω)	R_{ct} (Ω)
Bp-Si	10.76	7.62×10^{-8}	-	-	-	1.12×10^{6}
Co-P/Bp-Si	18.57	1.24×10^{-7}	304.9	3.59×10^{-4}	157.2	462.1
Ni-P/Bp-Si	13.83	1.23×10^{-7}	327.4	1.14×10^{-5}	361.5	688.9
Fe-P/Bp-Si	9.58	1.08×10^{-6}	278.5	1.12×10^{-4}	1176	1454.5

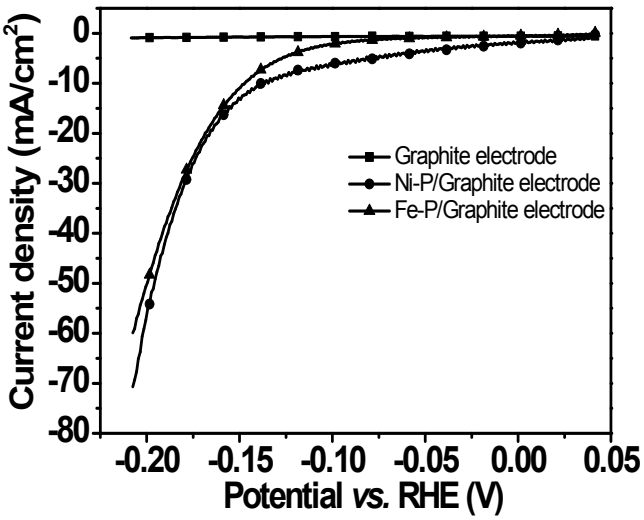

Fig. S12 Current-potential curves of graphite electrode, Ni-P/graphite electrode, and Fe-P/graphite electrode in 0.5 M H_2SO_4 solution with iR correction.

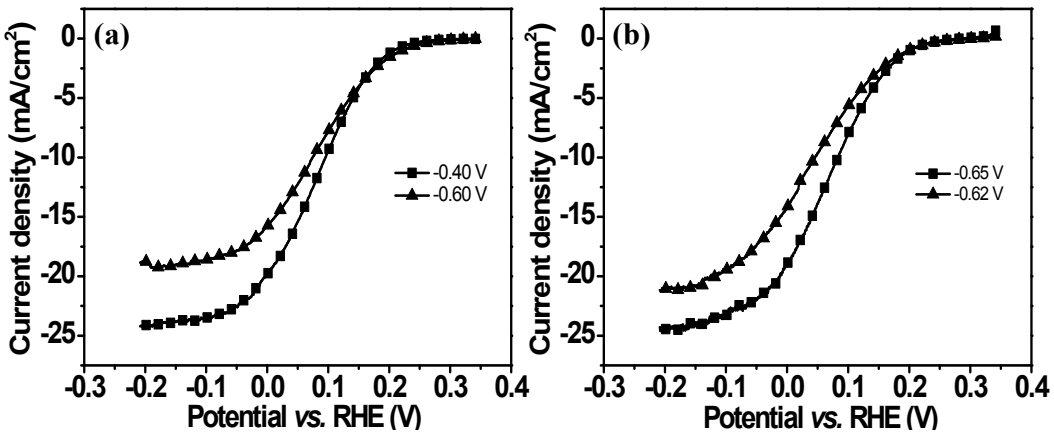

Fig. S13 Current-potential curves of (a) Ni-P/Bp-Si, and (b) Fe-P/Bp-Si prepared at different deposition potential (*vs.* SCE). Experimental details were presented in Fig. S14.

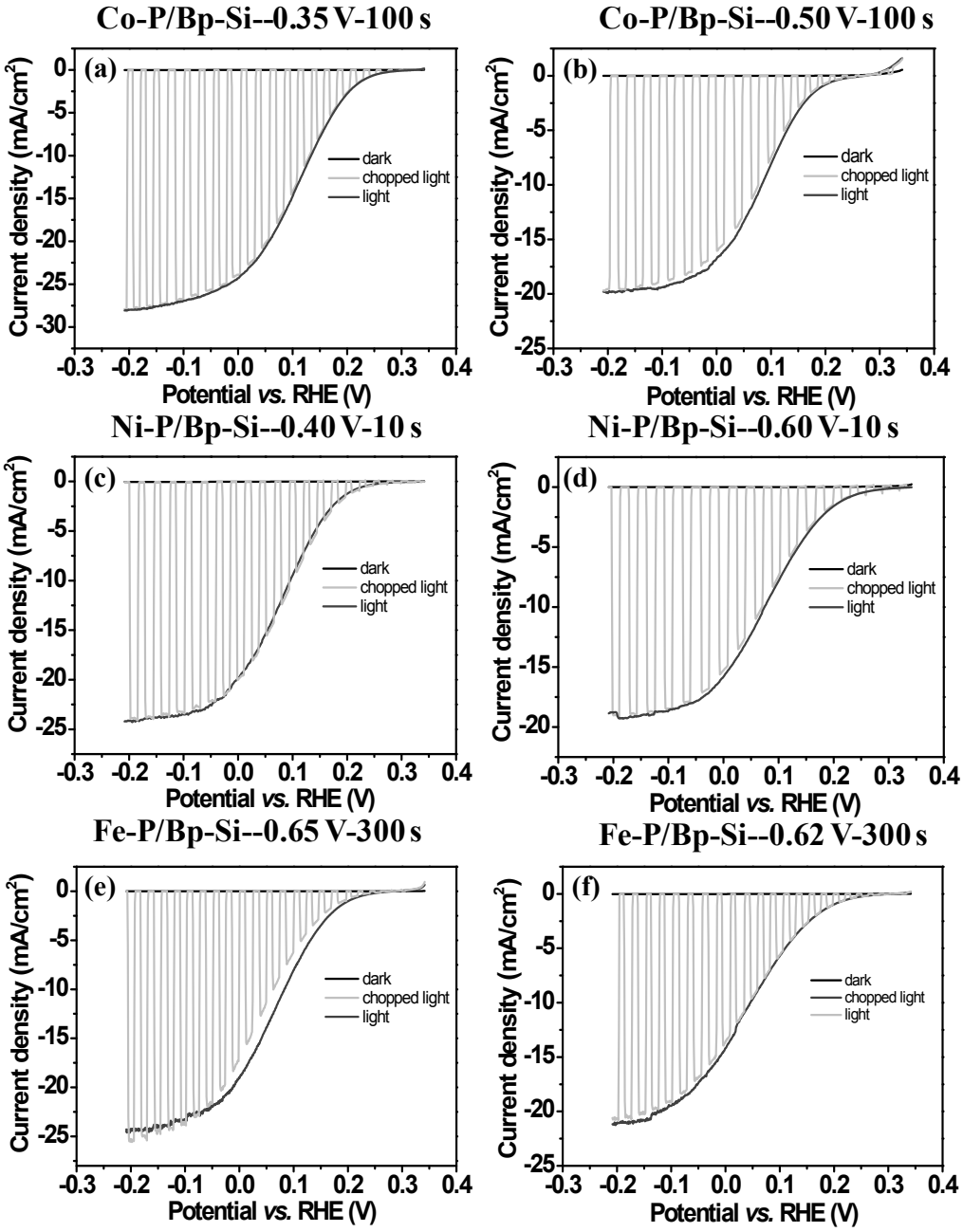

Fig. S14 M-Ps/Bp-Si prepared by photo-assisted electrodeposition in a plating solution at a certain bias (*vs.* SCE) for a certain time was denoted as M-P/Bp-Si-potential-time. For example, Co-P/Bp-Si--0.35 V-100 s meant it was prepared at an applied bias of -0.35 V *vs.* SCE for 100 s. (a)-(f) were polarization J-V curves of M-P/Bp-Si-potential-time at dark, chopped light and light conditions in 0.5 M H_2SO_4 solution under AM 1.5G illumination (100 mW cm^{-2}). Current-potential curves of (a) Co-P/Bp-Si--0.35 V-100 s, (b) Co-P/Bp-Si--0.50 V-100 s, (c) Ni-P/Bp-Si--0.40 V-10 s, (d) Ni-P/Bp-Si--0.60 V-10 s, (e) Fe-P/Bp-Si--0.65 V-300 s and (f) Fe-P/Bp-Si--0.62 V-300 s. Fig. 8a, Fig. S13, and Fig. S14 reflected the optimum deposition potentials of -0.35, -0.40, and -0.65 V *vs.* SCE for Co-P, Ni-P and Fe-P, respectively.

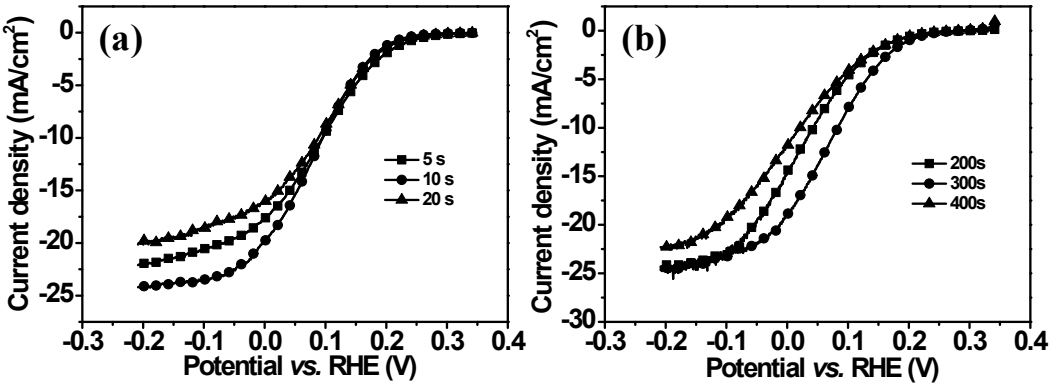

Fig. S15 Current-potential curves of (a) Ni-P/Bp-Si and (a) Fe-P/Bp-Si prepared at different deposition time. Experimental details were presented in Fig. S16.

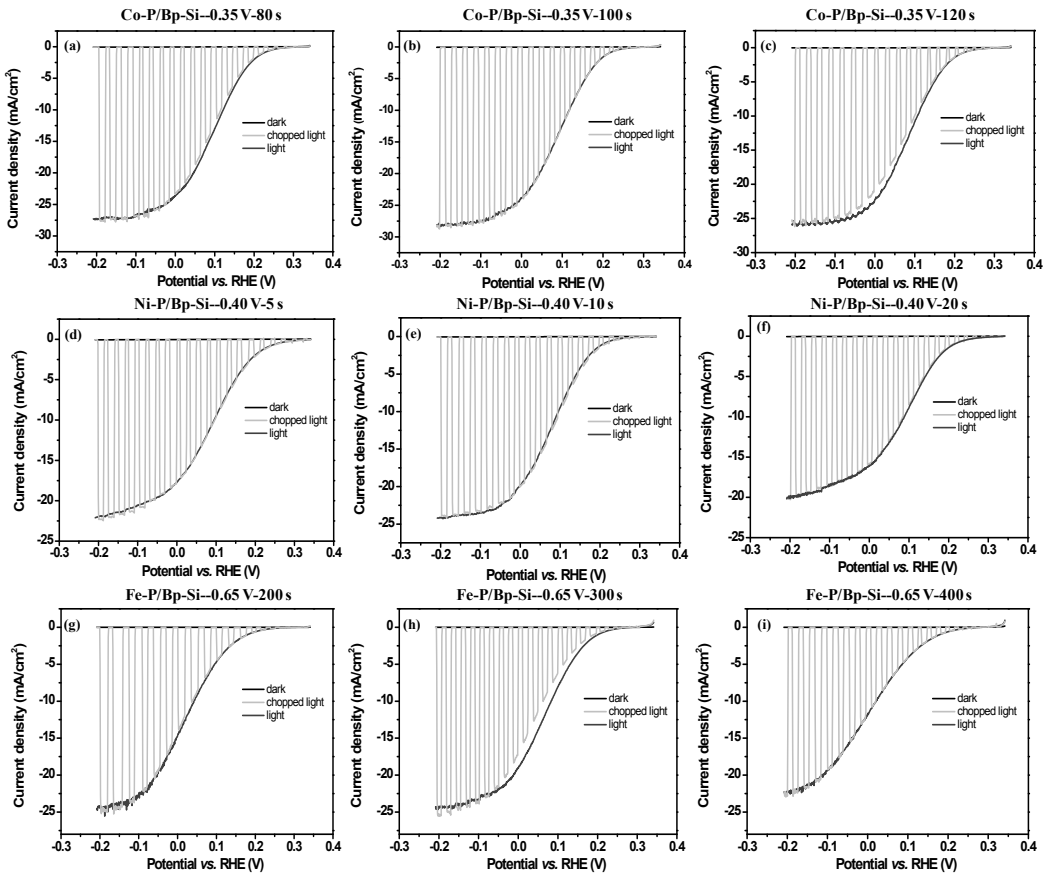

Fig. S16 M-P/Bp-Si prepared by photo-assisted electrodeposition in a plating solution at a certain bias (*vs.* SCE) for a certain time was denoted as M-P/Bp-Si-potential-time. For example, Co-P/Bp-Si--0.35 V-100 s meant it was prepared at an applied bias of -0.35 V *vs.* SCE for 100 s. Current-potential curves of (a) Co-P/Bp-Si--0.35 V-80 s, (b) Co-P/Bp-Si--0.35 V-100 s, (c) Co-P/Bp-Si--0.35 V-120 s, (d) Ni-P/Bp-Si--0.40 V-5 s, (e) Ni-P/Bp-Si--0.40 V-10 s, (f) Ni-P/Bp-Si--0.40 V-20 s, (g) Fe-P/Bp-Si--0.65 V-200 s, (h) Fe-P/Bp-Si--0.65 V-300 s and (i) Fe-P/Bp-Si--0.65 V-400 s at dark, chopped light and light conditions in 0.5 M H_2SO_4 solution under AM 1.5G illumination (100 mW cm^{-2}). Fig. 8b, Fig. S15, and Fig. S16 reflected the optimum deposition time of 100, 10, and 300 s for Co-P, Ni-P and Fe-P, respectively.

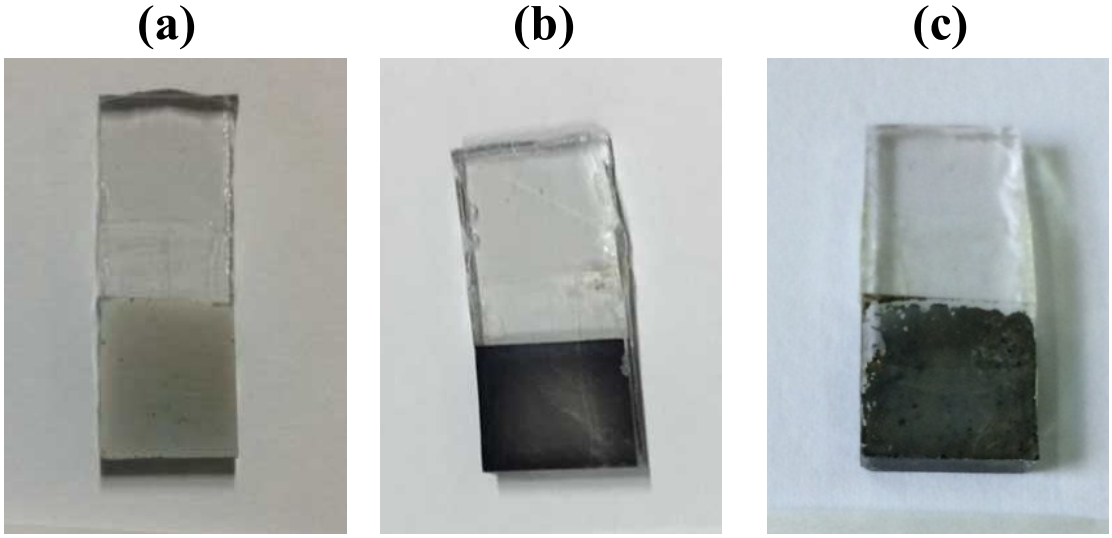

Fig. S17 Photographs of (a) Co-P/FTO, (b) Ni-P/FTO and (c) Fe-P/FTO prepared with an electrodeposition method for a long deposition duration. We can see that all the M-Ps cocatalysts are in deep color and therefore will hinder light absorption by the underlying Bp-Si if assembled on Bp-Si.

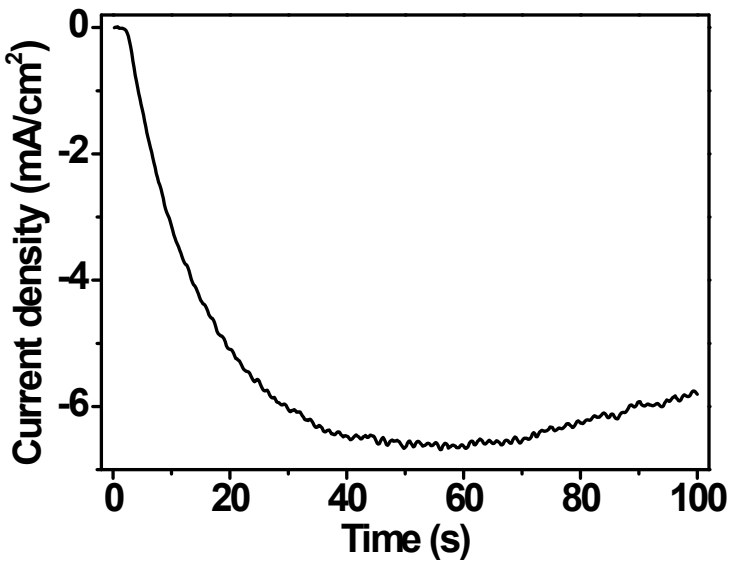

Fig. S18 The i-t curves for the photo-assisted electrodeposition of Co-P on Bp-Si at an applied bias of -0.35 V *vs.* SCE for 100 s under AM 1.5G illumination (100 mW cm^{-2}).

References

1 Z. Pu, Q. Liu, C. Tang, A.M. Asiri, X. Sun, *Nanoscale*, 2014, **6**, 11031-11034.

2 Y. Liang, Q. Liu, A.M. Asiri, X. Sun, Y. Luo, *ACS Catal.*, 2014, **4**, 4065-4069.

3 A.P. Grosvenor, S.D. Wik, R.G. Cavell, A. Mar, *Inorg. Chem.*, 2005, **44** , 8988-8998.

4 Y. Chen, P.D. Tran, P. Boix, Y. Ren, S.Y. Chiam, Z. Li, K.W. Fu, L.H. Wong, J. Barber, *ACS Nano*, 2015, **9**, 3829-3836.